

We have experimentally investigated the optical and electrical characteristics of a turbulent electric arc burning at the axis of a submerged jet.

The energy characteristics of plasmotrons with linear circuitry, in which the electric arc burns in a longitudinal stream of gas, are defined by the nature of the interaction between the arc and the flow of gas in the discharge chamber of the plasmotron. In a plasmotron with a partitioned interelectrode insert (IEI) and a supply of gas distributed through these sections to that segment of the channel exceeding  $a > 10-15d$  in length, we achieve a developed turbulent flow in which the turbulent heat and mass transfer exerts significant influence on all the characteristics of the electric arc [1]. In accordance with [2], the most characteristic features of the integral parameters in the case of a turbulent electric arc in the developed segments include the following: concentration of the current-conducting plasma in the near-axial zone; the independence of the time-average radius of the current-conducting cross section relative to the gas flow rate and the current strength; the possibility of precisely calculating the electric field strength ( $E \sim \sqrt{Re}$ ) by means of a channel model [3]. A shortcoming of the channel model [3] is the significant divergence (virtually by an order of magnitude) between the calculated radiant flux and that derived experimentally. Thus, the integral parameters of such a "turbulent" arc are in need of refinement and additional study, not to speak of local and pulsation characteristics with regard to which virtually no information exists. Obtaining experimental data with respect to an arc burning in a developed turbulent segment of gas flow in a closed cylindrical channel is associated with considerable technical difficulties [4]. For example, the application of tomography to produce temperature profiles within the arc column calls for the recording of spectral information from a large number of angles [5], and to obtain correlation characteristics of pulsations in temperature, conductivity, and strength, it is essential that these be measured simultaneously at various sections of the electroarc chamber.

It is the aim of the present paper to design such an electroarc installation in which the arc would burn in a turbulent jet flowing into open space and to study the characteristics of the current-conducting jet. A diagram of the experimental installation and the measurements is shown in Fig. 1. The plasmotron is made up of cathode 1, water-cooled IEI sections 2 with an inside diameter of  $d = 2 \cdot 10^{-2}$  m, with the overall assembly exhibiting a length of  $a = 14.5d$ . Air is fed into the gaps between the sections, with the rate of flow varying as  $\Sigma G_i = 5.9-30$  g/sec. The distribution of the flow rate through the IEI sections was kept uniform; the gas was twisted as it was fed into the first three intersectional gaps,

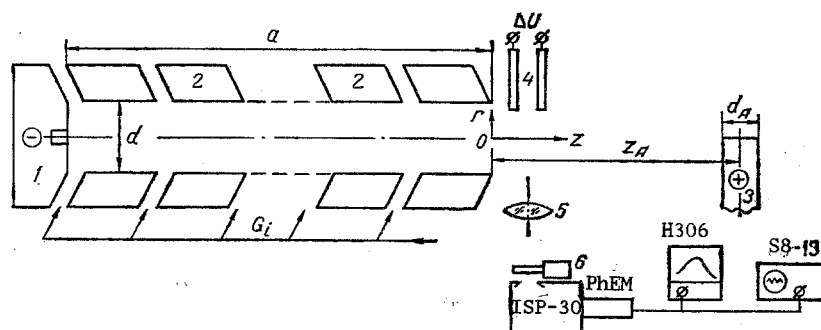


Fig. 1. Diagram of the experimental installation.

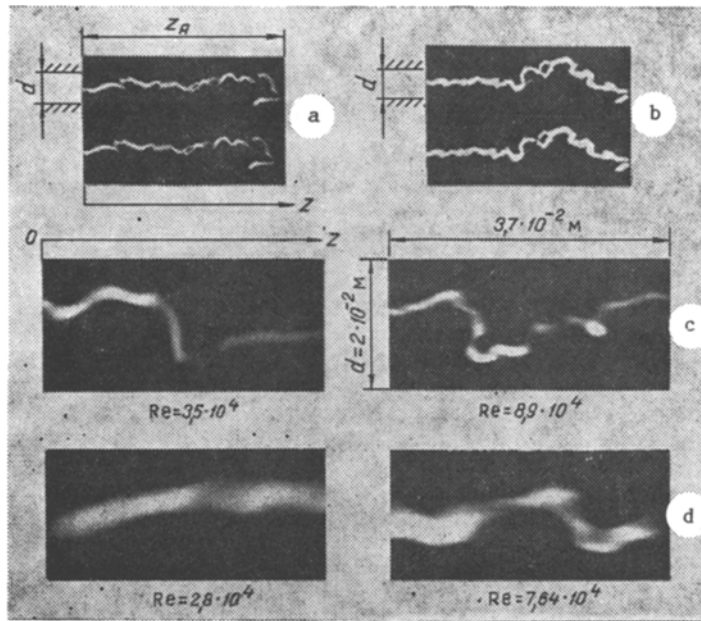


Fig. 2. Individual motion picture frames of the open segment of the turbulent arc: a, b)  $0 < z < z_A$ ,  $I = 150$  A,  $Re = 4.9 \cdot 10^4$ ; c)  $0 < z < 3.7 \cdot 10^{-2}$  m,  $I = 72$  A; d)  $0 < z < 3.7 \cdot 10^{-2}$  m,  $I = 200$  A;  $\tau_{\text{exp}} = 5.9 \cdot 10^{-6}$  sec.

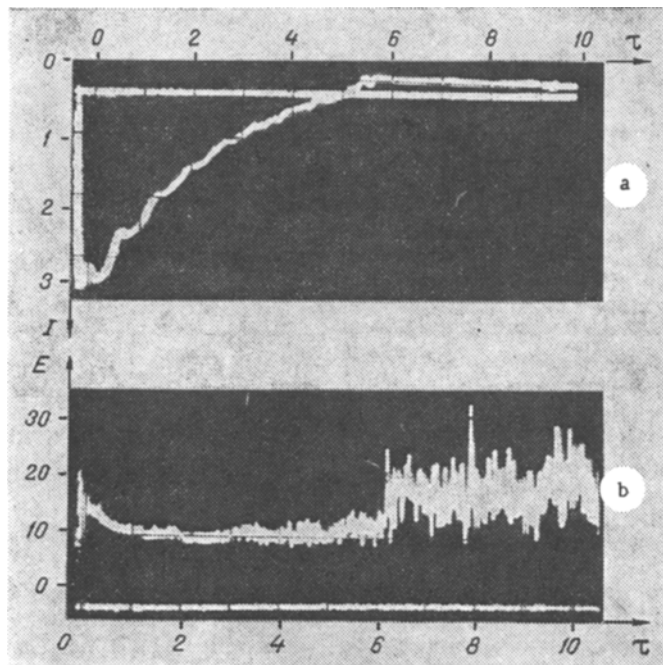


Fig. 3. Imposition of current pulse on quasisteady arc ( $I = 175$  A,  $Re = 3.5 \cdot 10^4$ ): a) oscillogram of current pulse; b) oscillogram of probe signal,  $\tau > 6$  msec, probe readings taken for combustion of quasisteady arc. E, V/cm; I, kA;  $\tau$ , msec.

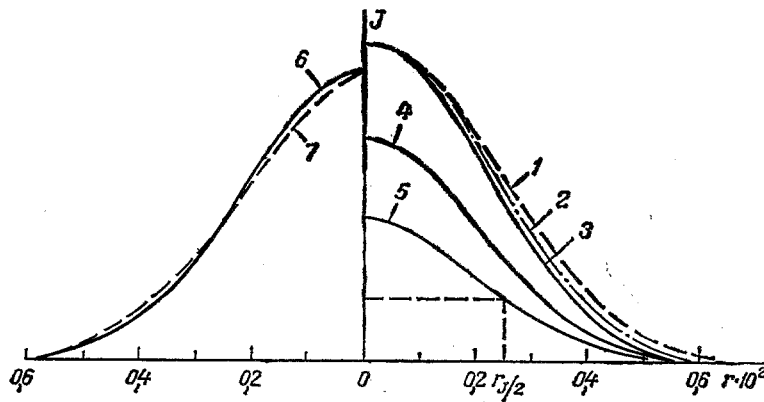


Fig. 4. Distribution of radiation intensity of the air arc along the radius at various lateral cross sections of the jet as a function of the Reynolds number and the arc current: 1)  $z = 4.5$  cm; 2) 2.5; 3) 0.5 for  $I = 200$  A,  $Re = 4.7 \cdot 10^4$ ; 4)  $I = 150$  A; 5) 100 for  $z = 0.5$  cm,  $Re = 4.7 \cdot 10^4$ ; 6)  $Re = 3.1 \cdot 10^4$ ; 7)  $10^5$  for  $I = 200$  A,  $z = 4.5$  cm.  $J$ , relative units;  $r$ , m.

and without any twisting to the remaining sections. The introduction of the gas in such a manner always insured a developed turbulent flow at the nozzle outlet of the IEI. The electric arc burns inside the IEI channel in a submerged jet and closes on the water-cooled vertically positioned cylindrical rod anode 3 with a diameter of  $d_A = 2.8 \cdot 10^{-2}$  m, whose axis was separated from the outlet section of the nozzle through a distance  $z_A = 7.5d$ .

During the course of the experiment, the electric-field strengths were measured along the length of the open arc segment by means of two tungsten probes 4. The wires had a diameter of  $2 \cdot 10^{-3}$  m, and they were separated by  $1 \cdot 10^{-2}$  m. The probe potential difference  $\Delta U$  was measured by means of a static S50 voltmeter or it was applied to the differential input of an S8-13 oscillograph. The radial distribution of the radiation intensity of the continuum at the wavelength  $\lambda = 393$  nm was recorded by means of a two-coordinate N306 automatic recording instrument. The radiation of the arc column in various cross sections of the jet was projected by means of lens 5 to the slit of the ISP-30 spectrograph and scanned along the radius by means of electromechanical device 6. The scanning time was 8 sec. Direction motion-picture photography of the open segment of the electric arc was accomplished by means of a high-speed VSK-5 camera.

Figure 2a, b shows the characteristic motion-picture frames (two successive frames) of the electric arc column for the segment between the anode and the outlet from the plasmotron nozzle. The single-frame exposure time for Fig. 2a is  $\tau_{\text{exp}} = 2.8 \cdot 10^{-6}$  sec, while that for Fig. 2b is  $5.28 \cdot 10^{-6}$  sec. The time elapsing between frames for Fig. 2a is  $0.56 \cdot 10^{-6}$  sec, while that for Fig. 2b is  $0.31 \cdot 10^{-6}$  sec. As we can see from the photography results, the deviations in the luminescent arc elements do not extend beyond the IEI channel radius up to distances no more than  $4d$  from the outlet section of the nozzle (Fig. 2b) or even over the entire length  $z_A$  (Fig. 2a).

The latest modifications of high-speed photography have made it possible to undertake studies which reveal the structure of the luminous emittance. Figure 2c,d show two series of motion-picture frames of the change in the shape of the electric arc while the current is kept constant, and for two values of the number  $Re = 4G/(\pi d \mu)$ , determined from the cold-air parameters at the outlet section from the plasmotron channel. The photography was conducted over a segment exhibiting a length of  $3.7 \cdot 10^{-2}$  m.

Analysis of a large quantity of motion-picture frames also reveals the following: over the entire range of arc current and Reynolds numbers the deviations in the luminescent segments of the arc in the radial direction do not extend beyond the limits of some jet radius  $r \leq (0.5-0.6)d/2$ ; the increase in the Reynolds number for a fixed arc current leads to the appearance of smaller-scale nonuniformities in the luminous emittance; an increase in the arc current intensifies the uniformity of arc-column luminescence as a whole. This latter circumstance is apparently associated with the increasing role played by radiation heat exchange in the process of energy transfer, which in the final analysis leads to complete even-  
ing out of the temperature field and to a situation in which the arc column assumes an axisym-

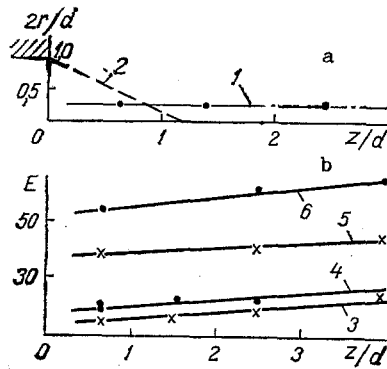


Fig. 5. Change in the boundary of the current-conducting zone and the time-averaged strength of the electric field of the arc along the axis of the jet: a) curve 1 -  $r_{J/2} = f(z/d)$  for the case in which  $I = 100-200$  A,  $Re = (2-10) \cdot 10^4$ ; curve 2 - the radius of the inside boundary of the displacement zone on discharge of the nonisothermal submerged jet of air out of the nozzle (calculation in accordance with [6]); b)  $E = f(z/d)$ ; 3 -  $I = 200$  A; 4 -  $I = 100$  A for  $Re = 2 \cdot 10^4$ ; 5 -  $I = 200$  A; 6)  $I = 100$  A when  $Re = 9 \cdot 10^4$ .

metric shape. In the case of large currents, this must lead to a significant reduction in the pulsations of electric-field strength and luminous emittance. The foregoing is confirmed by a number of experiments that are preliminary in nature and have been carried out by the authors in conjunction with A. D. Lebedev and A. P. Plyushkin. A pulse of current was applied from a capacitor battery in these experiments to a steadily burning arc. Simultaneously, oscillograms were recorded for the current with Rogovskii bands (or shunts) or the signal from the probes (Fig. 3). The signal from the probes was recorded at the section  $z = 0.75d$ . As the current was reduced from 2-4 kA to values of 800-600 A the variations in field strength are virtually absent, and subsequently they increase to the values prevailing in a quasi-steady burning arc. The variable component in the latter case amounts to  $\pm 50\%$  of the average value of  $\Delta U$ ; the frequencies of the large-scale pulsations are on the order of  $10^3$  Hz, while those of the small-scale pulsations are greater than  $10^4$  Hz. Analysis of the oscillograms for the pulsation components of continuum radiation intensity in the case of  $\lambda = 393$  nm, reflecting the time variation of the radiant flux, gathered over the entire lateral cross section of the arc flow through the width of the slit of the spectrograph shows that the characteristics of oscillation frequencies in the case of radiation and oscillations in the strength of the electric field are close to one another. From all appearances, the integral gradient flux through the cross section of the discharge and the integral conductivity in that same cross section depend identically on variations in the temperature field. A more precise answer can be found only through correlation analysis. The integral distribution over time along the radius of radiation intensity for the air arc in the case of the continuum  $\lambda = 393$  nm can be found in Fig. 4. Curves 1-3 show that various distance from the outlet section of the plasmotron (to distances of  $z/d = 2.25$ ) have little effect on the nature of the distribution, and the 3.5-fold change in the air flow rate (curves 6 and 7) also exerts little influence. If we take the radius  $r_{J/2}$  (see Fig. 4) as the characteristic of the arc-channel boundary, at which the intensity of the continuum radiation is reduced by a factor of two relative to its value at the axis of the arc, this boundary over the length of the jet expands only slightly for the entire investigated range of experimental data (curve 1, Fig. 5a). At the same time, the flow which we are examining here is an example of a case of jet gas escape into a nonmoving space, i.e., the case of a somewhat specifically submerged jet. For jets free of current we know of quantitative relationships governing the behavior of the displacement boundaries; Fig. 5a (curve 2) shows the estimated value of the inside displacement boundary, calculated in accordance with the recommendations of [6] for the conditions of discharge for the submerged jet of air out of the nozzle with minimum nonuniformity in the initial distributions of the jet parameters and in the ratio of discharge-current densities  $\rho_1$  to that of the unperturbed gas  $\rho_2$ ,  $n = \rho_2/\rho_1 = 7.25$ . In our case, this ratio varied from 8 to 25, i.e., the initial segment of the jet must be even shorter. In other words, the mixing of the ambient cold air must occur at some small distance from the outlet section of the plasmotron nozzle over the entire cross section of the jet.

The drawing-in of the ambient air first of all affects the distribution of the electric-field strength along the jet. This can be observed in analysis of the volt-ampere characteristics of the arc in the open segment. In the range of currents under consideration these characteristics are descending, which is typical of a turbulent electric arc. In comparing the function  $E = f(I)$  calculated on the basis of the "channel" model, we find that the curves are situated slightly below those representing the experiment and are equidistant from the latter, i.e., a functional relationship of the  $E \sim \sqrt{Re}$  type is also retained for the open turbulent arc, while the divergence of the curves is explained by the influence exerted by the connected flow rate and the concurrent increase in the  $Re$  numbers.

The change in the intensity of the electric field along the open portion of the arc can be seen in Fig. 5b. The quantity  $E$  increases linearly with increasing distance from the outlet section of the plasmotron nozzle; however, this increase is only slight and amounts to 3-4 V/cm or 10-20% relative to the intensity of the field at the outlet section. As can be seen from Fig. 5a, since the dimension of the conducting core undergoes virtually no change, the increase in  $E$  can be associated with the increase in the Reynolds number that comes about by connection to the mass from the external medium. It is possible to evaluate the magnitude of this mass or the so-called connected flow rate of the jet under the condition that  $E \sim \sqrt{Re}$  is satisfied, as well as to satisfy the condition of proportional increase in the  $Re$  number with an increase in the connected flow rate:

$$\Delta G = G(z)/\Sigma G_i.$$

Here  $G(z)$  is the total rate of flow through the cross section of the jet. For submerged jets we know that the magnitude of the connected flow rate increases linearly with increasing distance from the nozzle, i.e.,  $\Delta G = Kz$ . The coefficient  $K$  depends on the conditions of flow. In particular, for the initial segment of the jet discharging out of the long cylindrical channel, which is very nearly the same as the flow which we are considering here, we have  $K = 0.183$  [7]. For those jets being discharged into submerged space out of short nozzles we have  $K = 0.03-0.61$  [6], where the smaller value corresponds to  $n = 0.27$  (freon in air), and the larger value corresponds to  $n = 8$  (helium in air). For our conditions the estimate of  $\Delta G$  with consideration of all of the foregoing yields the following values:  $K = 0.17-0.06$ , with the higher value of  $K$  corresponding to the lower values of the  $Re$  numbers, while the lower value corresponds to  $Re \approx 10^5$ . Thus, the presence of an electric arc in a submerged jet leads to a situation in which the displacement intensity at the initial segment is reduced in comparison to jets of varying density without currents.

The results of these studies show that the parameters of an electric arc burning in a developed turbulent jet, which is discharged into submerged space, even with considerable distance from the outlet section of the channel, changes only slightly. What we have is an apparent "freezing-in" of the time-averaged temperature field, while the structure of the conducting arc channel and the exchange of heat between the arc and the gas flow are close to the values in the electric discharge chamber of the plasmotron. All of this allows us to use a long open turbulent arc with a linear face no smaller than  $(2-4)d$ , burning in a submerged jet, as a physically adequate model of turbulent electroarc flow in a plasmotron channel, convenient for purposes of diagnosis.

#### NOTATION

$r, z$ , radial and axial coordinates;  $a$ , length of the partitioned IEI of the plasmotron;  $d$ , diameter;  $z_A$ , distance from the outlet section of the IEI to the axis of the extended anode;  $d_A$ , diameter of the extended anode;  $E$ , strength of the electric field;  $I$ , arc current;  $\Delta U$ , probe potential difference;  $J$ , radiation intensity;  $\lambda$ , radiation wavelength;  $G$ , flow rate of the gas;  $Re$ , Reynolds number;  $\mu$ , viscosity;  $\rho$ , density;  $\Delta G$ , connected jet flow rate.

#### LITERATURE CITED

1. M. F. Zhukov, A. S. An'shakov, I. M. Zasyepkin, et al., Electroarc Generators with Inter-electrode Inserts [in Russian], Novosibirsk (1981).
2. B. A. Vryukov and A. É. Fridberg, Izv. SO Akad. Nauk SSR, Ser. Tekh. Nauk, No. 8, Issue 2, 3-6 (1972).
3. M. F. Zhukov, V. P. Lukashov, B. A. Pozdnyakov, and N. M. Shcherbik, Inzh.-Fiz. Zh., 50, No. 3, 357-362 (1986).

4. M. F. Zhukov, I. M. Zasyplin, and Yu. S. Levitan, *Izv. SO Akad. Nauk SSSR, Ser. Tekh. Nauk*, No. 11, Issue 3, 25-51 (1987).
5. M. F. Zhukov, T. S. Mel'nikova, V. V. Pikalov, and N. T. Preobrazhenskii, *Izv. SO Akad. Nauk SSSR, Ser. Tekh. Nauk*, No. 10, Issue 2, 17-24 (1982).
6. G. N. Abramovich (ed.), *Turbulent Mixing of Gas Jets [in Russian]*, Moscow (1974).
7. L. Boguslawski and Gz. O. Popiel, *J. Fluid Mech.*, 90, Pt. 3, 531-539 (1979).

#### STUDYING UNSTABLE REGIMES OF JET INTERACTION WITH APPROACHING FLOWS

V. V. Kondrashov and R. I. Soloukhin\*

UDC 533.6.011

We present and clarify results from numerical experiments pertaining to the description of unstable flow regimes where supersonic jets are propagated into an oncoming gas flow.

Problems of propagation in media and the interactions between these media and supersonic gas jets are of considerable interest. Here, results of studies into the nonsteady (unstable) regimes of flow in the oppositely directed interaction of an underexpanded heated supersonic jet with a flow have not been systematically organized and they are frequently contradictory [1-3]. This is associated with the considerable difficulties involved in deriving information regarding specific details of the flow in an instrumental study of the spatial pulsating flows which can frequently be obtained during the course of numerical experiments with a computer, and these difficulties arise also as a consequence of the great sensitivity of the flows in the case of unstable regimes to minor variations in the determining parameters.

Even the initial attempts to utilize profiled subsonic nozzles for purposes of generating sonic jets streamlining a surface turned into the direction of the flow gave evidence of an extremely complex interaction between the parameters defining the flow of the gas within the nozzle and the streamlining [by an external flow] of a body with a notched nozzle in its nose section [1, 4].

At the beginning of the 1960s researchers demonstrated that a flow is nonsteady if the total pressure across the jet is small and if the characteristic dimension of the jet is small in comparison with the dimensions of the body. The oncoming jet in this case is regarded as a gasdynamic analog of a needle or a cone, mounted on the forward section of a body, and the results of investigations into the latter, both here and abroad [5], were applied to this approaching stream. Unstable interaction regimes (UIR) of a jet with a flow in this case is characterized by the conditions under which the separated region is formed at the surface and by the mutual disposition of the deformed bow shock and the body.

The forces assumed in [6] for the development of an analytical model of oncoming jet interaction with a flow demonstrated the importance of making provision for the regimes under which a jet is discharged out of a nozzle, and the related UIR. Results from studies into these interaction regimes, making provision for the extent to which the calculations for the jet are incomplete, have been generalized in [7], where an attempt was also undertaken to construct a model to determine the parameters in the region of the detached flow. The accumulated data from these experimental studies showed that the UIR are determined also by the conditions of flow for the jet layer near the point at which the detached region closes. In this case, the very presence of a mass source within the flow becomes significant.

---

\*Deceased.

---

A. V. Lykov Institute of Heat and Mass Exchange, Academy of Sciences of the Belorussian SSR, Minsk. Translated from *Inzhenerno-Fizicheskii Zhurnal*, Vol. 57, No. 4, pp. 539-545, October, 1989. Original article submitted May 16, 1988.